Scientific Reports

https://doi.org/10.1038/s41598-026-49541-9

Article in Press

HSN G1 demonstrates multifaceted therapeutic strategy against Alzheimer disease in APP PS1 mouse model

Received: 2 April 2025

Accepted: 15 April 2026

Published online: 22 April 2026

Cite this article as: Ahn J.W., Yoon E., Kim H.S. *et al.* HSN G1 demonstrates multifaceted therapeutic strategy against Alzheimer disease in APP PS1 mouse model. *Sci Rep* (2026). https://doi.org/10.1038/s41598-026-49541-9

Jeong Won Ahn, Eun-Jung Yoon, Hyun Soo Kim, Yunseo Choi, Jiwon Jeong, Kongara Damodar, Yeong-Min Yoo, Dongsun Park & Seong Soo Joo

HSN G1 demonstrates multifaceted therapeutic strategy against Alzheimer disease in APP PS1 mouse model

Jeong Won Ahn[1†], Eun-Jung Yoon[2†], Hyun Soo Kim[1], Yunseo Choi[3], Jiwon Jeong[3], Kongara Damodar[4], Yeong-Min Yoo[1,5], Dongsun Park[6*], and Seong Soo Joo[1,4*]

[1]College of Life Science, Gangneung-Wonju National University, 7 Jukheon-gil, Gangneung 25457, Gangwon, Republic of Korea

[2]Department of Life Sports Educator, Kongju National University, Kongju 32588, Chungnam, Republic of Korea

[3]Laboratory of Toxicology, College of Veterinary Medicine, Kangwon National University, Chuncheon, 24341, Gangwon, Republic of

[4]Huscion MAJIC R&D center, 331 Pangyo-ro, Seongnam 13488, Gyeonggi, Republic of Korea

[5]Environmental Research Institute, Kangwon National University, Gangwon, Republic of Korea

[6]Laboratory of Toxicology, College of Veterinary Medicine, Kangwon National University, Chuncheon, 24341, Gangwon, Republic of Korea

[†]Equally contributed to this study

Authors information: Jeong Won Ahn, 0000@gwnu.ac.kr; Eun-Jung Yoon,

ejyoon@kongju.ac.kr; Hyun Soo Kim, k4609@gwnu.ac.kr; Yunseo Choi, yunseo0921@naver.com; Jiwon Jeong, yru0805@gmail.com; Kongara Damodar, kongaradamu@gwnu.ac.kr; Yeong-Min Yoo, yyeongm@hanmail.net

*Corresponding author

Dongsun Park, DVM, Ph.D

Laboratory of Veterinary Toxicology, College of Veterinary Medicine, Kangwon National University, 1 Kangwondaehak-gil, Chuncheon, Gangwon, 24341, Republic of Korea.

Mobile: +82-10-4105-0893 Tel: +82-33-250-8676 email: dvmdpark@kangwon.ac.kr, ORCID: 0000-0001-6042-5949

Seong Soo Joo, Ph.D.

Department of Marine Bioscience, College of Life Science, Gangneung-Wonju National University, 7 Jukheon-gil, Gangneung 25457, Gangwon, Republic of Korea. Tel/Fax: +82 33-640-2856, email: ssj66@gwnu.ac.kr, ORCID: 0000-0003-3449-0645

Abstract

Current therapeutic approaches for Alzheimer's disease (AD) demonstrate limited efficacy and fail to address disease progression. In the present study, we present HSN-G1, a novel ginsenoside-enriched pharmaceutical formulation that employs a dual-target mechanism through the modulation of amyloid clearance pathways and cholinergic neurotransmission. HSN-G1 demonstrates a reproducible ginsenoside profile enriched with Re (33.27 mg/g), Rd (25.00 mg/g), and Rg3 stereoisomers (12.18 mg/g), ensuring pharmaceutical-grade reproducibility. HSN-G1 enhanced amyloid-beta (Aβ) clearance in microglial cells, with significantly greater effects observed in SRA-overexpressing cells, suggesting SRA-dependent clearance mechanisms. In APP/PS1 transgenic mice, six-week oral administration of HSN-G1 (100–400 mg/kg) elicited significant dose-dependent improvements in cognitive performance. Male mice exhibited more stable and consistent enhancements in both passive avoidance and spatial memory tests compared to vehicle controls ($p < 0.001$), while both sexes demonstrated comparable reductions in brain Aβ levels (approximately 45%) and differential increases in acetylcholine (73% in males; 55% in females, $p < 0.01$). HSN-G1 administration enhanced the expression of neurotrophic factors, with NGF upregulation predominantly observed in males, whereas BDNF, CNTF, and GDNF were consistently elevated across both sexes. These findings establish HSN-G1 as a promising disease-modifying agent with standardized composition and therapeutic efficacy, surpassing the limitations of conventional single-

target approaches. The superior efficacy of HSN-G1 compared to existing treatments validates its potential for clinical development, highlighting the significance of sex-specific therapeutic responses in future AD therapeutics.

Keywords: Alzheimer's disease, Amyloid-beta, Neuroprotection, Cognitive function, APPswe/PS1dE9 mice, Microglial activation

1. Introduction

Alzheimer's disease (AD) represents one of the most pressing challenges in global healthcare, characterized by progressive cognitive decline and profound effects on patients, families, and healthcare systems (Gaugler et al., 2014; Sun et al., 2018). The complex pathogenesis of AD, involving amyloid-beta (Aβ) accumulation, tau pathology, neuroinflammation, and vascular dysfunction, necessitates therapeutic approaches that can address multiple pathological mechanisms simultaneously (Peng et al., 2023; Zhang et al., 2023). This complexity is further compounded by significant sex differences in AD prevalence and progression, with women comprising approximately two-thirds of AD patients—a disparity attributed not only to longer life expectancy but also to sex-specific variations in disease mechanisms and risk factors (Rahman et al., 2019).

Current therapeutic strategies for AD have shown limited success, primarily focusing on single targets and providing only symptomatic relief without effectively modifying disease progression (Passeri et al., 2022). Cholinesterase inhibitors such as donepezil and rivastigmine offer only temporary cognitive improvements, while memantine provides limited benefits restricted to moderate-to-severe patients. Recently approved antibody therapies (aducanumab, lecanemab) present challenges including cost burden, risk of cerebral edema, and requirement for frequent intravenous administration. These limitations of single-target

medications underscore the need for novel approaches capable of addressing multiple pathological mechanisms (Lane et al., 2018; Peng et al., 2023).

Natural compounds have emerged as promising candidates in this context, offering diverse biological activities including antioxidant, anti-inflammatory, and neuroprotective effects (Carregosa et al., 2020; Phan et al., 2019; Szwajgier et al., 2017; Thapa & Carroll, 2017). However, natural product-based drug development typically faces three major challenges: molecular complexity, difficulties in deconvoluting molecular mechanisms, and ensuring consistent quality. These barriers have significantly limited the advancement of natural product-based therapeutics in modern pharmaceutical development pipelines.

Among these natural compounds, ginsenosides from Panax ginseng have demonstrated particular promise through their ability to inhibit Aβ accumulation and modulate neuroinflammatory responses (Cao et al., 2016; Fang et al., 2012; Paik et al., 2023; Yang et al., 2021; Zhang et al., 2021). Specifically, certain ginsenosides including Re, Rd, and Rg3 individually exhibit potent neuroprotective and cognitive-enhancing properties (Cao et al., 2016; Fang et al., 2012; Yang et al., 2021; Zhang et al., 2021), yet exploration of their optimal combination for potential synergistic effects has been limited. In this context, we developed HSN-G1, a novel Re/Rd/Rg3-ratiometric formulation optimized through systematic molecular ratio studies. Our preliminary studies indicated that

this formulation exhibited significant neuroprotective effects and modulated key neurological pathways relevant to AD pathology (Ahn et al., 2021; Jang et al., 2015; Yoon et al., 2023).

In this study, we utilized the APPswe/PS1dE9 (APP/PS1) double-transgenic mouse model, which mimics key aspects of human AD pathology, to investigate the therapeutic potential of HSN-G1. This model is particularly valuable as it manifests both cholinergic system dysfunction and microglial activation abnormalities central to AD progression (Dong et al., 2019; Guo et al., 2020). Our experimental design incorporates both male and female animals to address potential sex-specific variations in disease progression and treatment responses (Waters & Laitner, 2021).

We hypothesized that HSN-G1, through its unique ginsenoside profile and standardized preparation, could provide a more effective and comprehensive approach to AD treatment compared with current options (Jiang et al., 2012). Our investigation focused on three key aspects: (1) characterization and standardization of HSN-G1 molecular composition, addressing the consistent quality issue that represents one of the major barriers in natural product-based drug development, (2) evaluation of its effects on both cholinergic function and microglial activation, elucidating its complex mechanisms of action, and (3) assessment of sex-specific therapeutic responses with potential mechanistic implications. This study aims to establish HSN-G1 as a novel therapeutic agent that addresses multiple AD pathological mechanisms while accounting for sex-specific

variations in treatment response, potentially offering a more effective approach to long-term AD management.

2. Materials and methods

2.1. HSN-G1 and Aβ42 sample preparation

The HSN-G1 compound was obtained from HUSCION Co., Ltd. (Gyeonggi, Republic of Korea). This preparation underwent our patented enrichment process (Patent No. US11622983B2) designed to optimize the ratio of active ginsenosides Re, Rd, and Rg3. The optimal ginsenoside ratio was determined based on established neuroprotective mechanisms: Rg3 promotes Aβ clearance through SRA-mediated phagocytosis and caveolin/clathrin-dependent pathways (Jang et al., 2015) and M2 microglial polarization for non-amyloidogenic processing (Ahn et al., 2021), while the combination with Re and Rd provides synergistic cognitive improvement (Yoon et al., 2023). The compound was stored at -20°C under a nitrogen atmosphere to ensure long-term stability. The optimal dosages (100, 200, and 400 mg/kg) were determined through preliminary dose-finding studies conducted over 2-4 weeks in C57BL/6 mice (n=6/group), which demonstrated dose-dependent cognitive improvements without toxicity (Yoon et al., 2023). Our dose-response optimization showed that 2 mg/kg donepezil achieved optimal cognitive enhancement (Morris water maze: escape latency reduced by 45±8%, $p<0.01$) with minimal adverse effects, while higher doses (5 mg/kg) caused significant weight loss (>15%) and behavioral abnormalities in aged APP/PS1 mice (detailed dose-

response data in Table S2) (Dong et al., 2009). For animal administration, HSN-G1 was dissolved in saline and prepared fresh immediately before use to preserve its integrity. Human amyloid-beta 42 (Aβ42) peptides, sourced from Eurogentec (Seraing, Belgium), were dissolved in anhydrous dimethyl sulfoxide (DMSO; Sigma-Aldrich, St. Louis, MI, USA) to achieve a concentration of 10 mM. The solution was sonicated for 4 min to ensure homogeneity and then diluted to a final concentration of 1 mM in cell culture medium. The diluted Aβ42 peptides were incubated at 4°C for 7 days before application according to established protocols (Klein et al., 2001). Donepezil hydrochloride (2 mg/kg), provided by Sigma-Aldrich, served as a comparative control. This dose was selected based on previous efficacy studies in APP/PS1 mice (Dong et al., 2009) and in vitro studies using 1 μM concentration (Takada-Takatori et al., 2019).

2.2. High-performance liquid chromatography (HPLC)

HPLC analysis was performed using an UltiMate 3000 HPLC system (Thermo Fisher Scientific, Waltham, MA, USA) comprising a vacuum degasser, quaternary pump, column, and an autosampler. Chromatographic separation was performed on a YMC-Triart C18 column (250 × 4.6 mm, 5 μm; YMC, Kyoto, Japan). The mobile phase comprised solvent A (water) and solvent B (acetonitrile). The following gradient elution program was used: 0–10 min (21–22% B), 10–11 min (22–23% B), 11–29 min (23–24% B), 29–34 min (24–30% B), 34–44 min (30–32% B), 44–49 min (32–50% B), 49–64 min (50–65% B), and 64–78 min (65–100% B) at

a flow rate of 1.6 mL/min. The column temperature was maintained at 30°C. A 10 µL sample was injected and the detection wavelength was set at 203 nm. The retention times (RTs) and peak areas of the ginsenoside peaks were logged using the Chromeleon software (version 7.2.10; Thermo Fisher Scientific). Each peak was identified by comparing its RT and ultraviolet spectra to that of a ginsenoside standard mixture (Biopurify Phytochemicals, Chengdu, China).

2.3. Cell culture

Human microglial HMO6 cells were kindly provided by Professor James YB KIM (Chungbuk National University). HMO6 cells and HMO6 cells stably overexpressing scavenger receptor A (HMO6.SRA) were cultured in Dulbecco's Modified Eagle's Medium (DMEM; Corning, NY, USA) supplemented with 10% fetal bovine serum (FBS; Corning) and antibiotics (100 U/mL penicillin and 100 µg/mL streptomycin; Corning) at 37°C in a humidified atmosphere containing 5% CO_2—the HMO6.SRA cell line was generated by lentiviral transduction as previously described (Jang et al., 2015). Cells were subcultured every 3-4 days using 0.25% trypsin-EDTA. To ensure optimal growth conditions and genetic stability, the cells were grown to >90% confluence and used within the first 20 passages for all experiments.

2.4. Cytotoxicity assay

Cytotoxicity was evaluated using the CytoTox 96 Non-Radioactive Cytotoxicity Assay Kit (Promega, Madison, WI, USA) with modifications

optimized for microglial cells according to our previous optimization study (Ahn et al., 2021). Briefly, HMO6 and HMO6.SRA cells were seeded at a density of 5×10^4 cells/well in 96-well plates and treated with various concentrations of HSN-G1 (100-400 μg/mL) or donepezil (1 μM) for 24 h. This assay measures the release of the lactate dehydrogenase (LDH) enzyme into the culture medium during cell lysis. Following treatment, 50 μL of cell culture supernatant was transferred to a new 96-well plate, to which 50 μL of the LDH reaction mixture was added. The plates were then incubated for 30 min at room temperature in the dark. Subsequently, the reaction was stopped using stop solution, and the absorbance of the resultant colorimetric product was measured at 490 nm using a microplate reader (Molecular Devices, San Jose, CA, USA), with background subtraction at 680 nm to correct for plate artifacts. Cytotoxicity was calculated as a percentage relative to maximum LDH release (100%) from cells completely lysed with the lysis buffer provided in the kit.

2.5. Assessment of Aβ removal

Aβ peptide was labeled with FITC using labeling kits (Thermo Fisher Scientific) to evaluate the efficacy of HSN-G1 in clearing Aβ. These peptides were dissolved in 1× phosphate-buffered saline (PBS) to reach a concentration of 5 mM and incubated at 37°C for 3 days to ensure proper conjugation and stability. HMO6 and HMO6.SRA cells were seeded at a density of 2×10^5 cells/well in 24-well plates containing poly-L-lysine-coated glass coverslips and allowed to adhere overnight. The cells were

then treated with varying concentrations of HSN-G1 (100, 200, or 400 μg/mL) or donepezil (1 μM) for 30 min, followed by exposure to 5 μM Aβ-FITC. Vehicle-treated cells exposed to Aβ-FITC served as the positive control, while untreated cells served as the negative control. After 24 h of incubation, cells were washed three times with PBS to remove extracellular Aβ-FITC, fixed with 4% paraformaldehyde for 15 min, and counterstained with DAPI to visualize nuclei. Cellular uptake and clearance of Aβ were visualized using an Evos FL Auto2 imaging system (Thermo Fisher Scientific) with appropriate filter sets for FITC and DAPI. For each condition, at least five random fields were captured, and fluorescence intensity was quantified using ImageJ software (NIH, Bethesda, MD, USA). The experiment was performed in triplicate.

2.6. Animal model

APP/PS1 transgenic mice (MMRRC strain #034832-JAX, The Jackson Laboratory, ME, USA) were selected based on their well-characterized AD pathology that closely mirrors human disease progression. They carry two AD-linked mutations: a chimeric mouse/human APP with the Swedish mutation (K670N/M671L) and a variant of human presenilin 1 (PS1) lacking exon 9, both linked to early-onset familial AD. In this model, amyloid plaques begin to appear in the cortex around 4 months and in the hippocampus by 6 months, growing in size and number over time (Jackson et al., 2013; Minkeviciene et al., 2008). These mice exhibit hallmark features of familial AD, such as Aβ accumulation in the brain,

neuroinflammation, and impairment of the cholinergic system, all of which contribute to cognitive deficits (Malm et al., 2011). Reflecting the higher prevalence of AD in female patients, this model also shows gender-specific pathological variations (Mielke, 2018; Onos et al., 2019; Ordóñez-Gutiérrez et al., 2015). The average body weight was 28.3 ± 2.1 g for males and 24.7 ± 1.8 g for females at the start of treatment. The breeding protocol maintained a ratio of one male to two females per cage. The experiments included wild-type (WT, eight-week-old) and transgenic siblings (twelve-month-old). The mice were housed in cages measuring 220 × 200 × 145 mm, with a strict policy of no more than four mice per cage to prevent overcrowding. The optimal laboratory conditions, including a constant temperature of 23 ± 2 °C, relative humidity of 55 ± 10%, 12-hour light/dark cycle, and a ventilation rate of 12 cycles/h, were controlled meticulously to provide a stable and stress-free environment and closely mimic the natural living conditions of the mice.

To evaluate the onset of dementia-like symptoms, mice aged approximately 12 months underwent cognitive assessments. Mice exhibiting significant cognitive deficits indicative of dementia were selected for further study. Cognitive assessments for animal selection included novel object recognition test and Y-maze spontaneous alternation test. Mice showing <50% preference for novel objects or <50% alternation were selected as cognitively impaired. The animals were randomly allocated to the following six groups: WT mice treated with saline as a vehicle, APP/PS1 mice treated with vehicle, and APP/PS1 mice treated with

donepezil at 2 mg/kg, or HSN-G1 at doses of 100, 200, and 400 mg/kg for six weeks. The treatment solutions were freshly prepared daily and administered orally at a dose of 10 mL/kg. All the experimental groups consisted of equal numbers of female and male mice (n = 6). Behavioral tests to assess the impact of HSN-G1 on learning and memory were conducted five weeks after treatment commencement. Following the six-week treatment period, the mice were euthanized for further analysis of AD hallmarks (Fig. 1A). Prior to euthanasia, all animals were anesthetized with isoflurane (2–3% for induction, 1.5–2% for maintenance) delivered in oxygen using a calibrated vaporizer to minimize pain and distress. Euthanasia was then performed by cervical dislocation under deep anesthesia, in accordance with the guidelines of the Institutional Animal Care and Use Committee (IACUC) at Chungbuk National University Animal Center (CBNUA-1398-20-01). All experiments followed ARRIVE guidelines and relevant animal care regulations.

2.7. Passive avoidance test

Passive avoidance test (PAT) was performed to assess memory enhancement in mice using a custom-designed shuttle box (ENV-010MD; Med Associates, St. Albans, VT, USA), as described in our preliminary study (Yoon et al., 2023). PAT is a widely recognized method for evaluating learning and memory in animal models and is especially pertinent to AD research because of its emphasis on associative memory processes (Fig. 1B). The shuttle box consisted of illuminated and dark compartments

separated by a guillotine door. The test was conducted over two consecutive days. On the first day (acquisition trial), each mouse was placed in the illuminated compartment facing away from the door and allowed to explore for 10 seconds. Then, the guillotine door was opened, allowing the mouse to enter the dark compartment. Once the mouse entered the dark compartment (with all four paws), the door was closed, and a mild foot shock (0.5 mA, 2 seconds) was delivered through the grid floor. The mouse was removed from the dark compartment 10 seconds after the shock and returned to its home cage. Twenty-four hours later (retention trial), the mouse was again placed in the illuminated compartment, and the latency to enter the dark compartment was recorded as a measure of memory retention, with a maximum cutoff time of 180 seconds. Longer latencies indicated better memory retention. The test was performed between 10:00 and 14:00 to minimize circadian influences, and the apparatus was cleaned with 70% ethanol between trials to eliminate olfactory cues.

2.8. Morris water maze test

Spatial memory was assessed using the Morris water maze test (MWMT) as described previously (Yoon et al., 2023). The test was conducted in a circular pool (120 cm diameter) filled with opaque water, with a submerged platform (10 cm diameter) in one quadrant. Mice underwent a 5-day acquisition phase (4 trials/day, 60-second maximum per trial) to locate the hidden platform using external visual cues. On day 6, a

60-second probe trial was conducted with the platform removed. Escape latency during training and time in target quadrant during the probe trial were recorded as measures of spatial learning and memory (Fig. 1C).

2.9. Brain tissue acetylcholine concentration

A detailed biochemical analysis was performed to accurately measure the concentration of acetylcholine (ACh), a critical neurotransmitter implicated in AD. Brain tissue was initially homogenized in nine-volumes of PBS containing a protease inhibitor cocktail (Sigma-Aldrich). Acetylcholine levels were then quantified using the Amplex Red Acetylcholine/ Acetylcholinesterase Assay Kit (Molecular Probes, Eugene, OR, USA), according to the manufacturer's instructions (Yoon et al., 2023).

2.10. Brain tissue Aβ concentration

Brain tissue Aβ42 concentrations were determined in the hippocampus and cortex. Tissues were homogenized in four-volumes of PBS containing protease inhibitor cocktail (Sigma-Aldrich), followed by centrifugation at 16,000 × g for 20 minutes at 4°C. The supernatant was collected for soluble Aβ analysis. Aβ42 levels were quantified using a human Aβ42 enzyme-linked immunosorbent assay (ELISA) kit (Invitrogen, Carlsbad, CA, USA). Results were normalized to total protein content and expressed as pg/mg protein (Park et al., 2020).

2.11. Western blot analysis

Brain tissues were lysed in radioimmunoprecipitation assay (RIPA) buffer supplemented with proteinase and phosphatase inhibitors (Sigma-

Aldrich). Protein concentration was determined using the BCA assay. Equal amounts of protein (30 μg) were separated on 10-15% SDS-PAGE gels and transferred to PVDF membranes. After blocking with 5% non-fat milk, membranes were incubated with primary antibodies overnight at 4°C, followed by HRP-conjugated secondary antibodies. Protein bands were visualized using an enhanced chemiluminescence (ECL) solution (Thermo Fisher Scientific), and signals were analyzed using ImageJ software (version 1.51j8; NIH, Bethesda, MD, USA). Other detailed procedures not described were referred to the previous experiments (Ahn et al., 2021; Park et al., 2020). Results are expressed as fold-change relative to the control group, with GAPDH as loading control. The specific antibodies used are listed in Table S1. Expression analysis of cholinergic transporters (CHT1 and VAChT) was performed using the same protocol, with detailed results presented in Table S4.

2.12. Immunohistochemical staining of brain tissues

Immunohistochemical staining was performed to assess specific protein expression within mouse brain tissues. Initially, the brains were fixed in a 10% formaldehyde solution and then embedded in 30% sucrose as a cryoprotectant to prepare for sectioning. Thin sections of 30 μm thickness were cut to ensure consistent sampling across all specimens. These sections were then incubated with primary antibodies targeting glial fibrillary acidic protein (GFAP; 1:300 dilution; Chemicon, Temecula, CA, USA) or Aβ (1:300 dilution; MyBioSource, San Diego, CA, USA) overnight

at 4°C. Next, the sections were incubated with Alexa Fluor-488 (for Aβ, 1:300 dilution; Molecular Probes, Eugene, OR, USA) or -594 (for GFAP, 1:300 dilution; Molecular Probes) secondary antibodies for 1 h at room temperature. The stained slides were imaged using the Evos FL Auto2 system. The captured images were then analyzed using the ImageJ software for a detailed analysis of protein expression and localization within brain tissues.

2.13. Acetylcholinesterase activity assay

Acetylcholinesterase activity in brain homogenates was measured using the Ellman colorimetric method with acetylthiocholine as substrate (Ellman et al., 1961). Detailed results are presented in Table S3.

2.14. Statistical analysis

Statistical analyses were performed using one-way ANOVA followed by Tukey's post-hoc test for multiple comparisons. Sample size was determined based on pilot studies (effect size d=1.8, α=0.05, β=0.2; detailed dose-response optimization in Supplementary Table S2). However, the small sample size (n=3/sex/group) limits statistical power and generalizability. Effect sizes (Cohen's d) and 95% confidence intervals were calculated for all comparisons. Data are presented as mean ± standard deviation. Significance levels: *$p < 0.05$, **$p < 0.01$, ***$p < 0.001$ versus WT control; #$p < 0.05$, ##$p < 0.01$, ###$p < 0.001$ versus vehicle-treated APP/PS1 mice. All analyses were conducted using SPSS version 12.0 with Bonferroni correction applied for multiple testing.

3. Results

3.1. Molecular Ratio Optimization and Characterization of HSN-G1

The optimal molecular ratio of HSN-G1 was established through systematic optimization studies evaluating different combinations of Re, Rd, and Rg3 (data not shown). The final Re/Rd/Rg3 ratio (33.27:25.00:12.18 mg/g) was selected based on our previous optimization studies (Jang et al., 2015; Ahn et al., 2021; Yoon et al., 2023). The ratio reflects the natural composition of fermented ginseng berry extract optimized through our standardized manufacturing process, which ensures batch-to-batch reproducibility of these bioactive components. HPLC analysis confirmed the reproducibility of this precise molecular composition (Fig. 2, Table 1), demonstrating batch-to-batch consistency with less than 5% variation. Method validation demonstrated excellent linearity ($r^2 > 0.999$), precision (intra-day CV < 2%, inter-day CV < 3%), and accuracy (recovery 98-102%) for all major ginsenosides. The stability of HSN-G1 was confirmed under various storage conditions (4°C, 25°C, 40°C/75% RH) for up to 12 months, with no significant degradation of active components. This standardized ratio distinguishes HSN-G1 from conventional formulations and establishes the foundation for its reproducible therapeutic effects through specific molecular targeting.

3.2. HSN-G1 enhances microglial Aβ clearance through SRA-dependent mechanisms

In both HMO6 and HMO6.SRA microglial cells, HSN-G1 treatment provided dose-dependent cytoprotection against Aβ-induced toxicity, as evidenced by a significant reduction in lactate dehydrogenase release ($p < 0.001$) (Fig. 3A). In particular, HMO6.SRA cells—which overexpress the scavenger receptor type A (SRA)—exhibited markedly lower cytotoxicity compared to HMO6 cells ($p < 0.001$), underscoring the critical role of SRA in mediating HSN-G1's neuroprotective effects. To further elucidate the mechanism, fluorescence microscopy was performed using FITC-labeled Aβ (applied at 5 μM and incubated for 4 h). HSN-G1 treatment at concentrations ranging from 100 to 400 μg/mL significantly enhanced Aβ clearance in both cell types (Fig. 3B). Quantitative fluorescence analysis revealed dose-dependent reduction in intracellular FITC-Aβ levels, with HMO6 cells showing 75% reduction and HMO6.SRA cells exhibiting significantly enhanced clearance with 92% reduction at 400 μg/mL compared to the Aβ control group ($p < 0.001$) (Fig. 3C). Notably, the Aβ clearance effect achieved by HSN-G1 was comparable to, or even exceeded, that observed with 1 μM donepezil, the current standard treatment. These results suggest that HSN-G1 enhanced Aβ clearance in microglial cells, with significantly greater effects observed in cells overexpressing SRA, suggesting SRA-dependent mechanisms.

3.3. Sex-specific responses in cognitive enhancement by HSN-G1 treatment

Six-week oral administration of HSN-G1 produced significant dose-

dependent improvements in cognitive performance, with notable sex-specific differences in response patterns. In the passive avoidance test, male mice showed more consistent improvements across all doses (ED50 = 157.3 ± 12.4 mg/kg), while female mice exhibited a steeper dose-response relationship (ED50 = 243.6 ± 18.7 mg/kg) (Fig. 4A-B). The sex-specific differences were particularly evident in the Morris water maze test, where male mice demonstrated superior spatial memory enhancement at lower doses (100-200 mg/kg) compared to females (Fig. 4C-D). The selection of HSN-G1 doses (100-400 mg/kg) was based on comprehensive dose-finding studies that demonstrated dose-dependent cognitive improvements without toxicity (Supplementary Table S2). Importantly, no adverse effects were noted during the treatment period, with all treatment groups maintaining stable body weight throughout the 6-week study (Fig. S1). Despite the small sample size, individual animal data demonstrated consistent treatment effects with low within-group variability (CV < 15% for most measures; Table S5), supporting the reliability of our findings

3.4. Differential regulation of cholinergic function

HSN-G1 treatment resulted in a dose-dependent elevation of brain acetylcholine (ACh) levels in both male and female APP/PS1 mice, as measured using the Amplex Red Acetylcholine/Acetylcholinesterase Assay (Fig. 5). Quantitative analysis revealed that male mice exhibited a 73% increase in ACh levels at the highest dose (400 mg/kg) compared to

vehicle-treated APP/PS1 controls ($p < 0.001$), while female mice showed a 55% increase ($p < 0.01$). This statistically significant sex-specific difference in cholinergic response may underlie the observed variations in cognitive performance stability, with enhanced cholinergic signaling in male mice potentially contributing to more consistent improvements in learning and memory. These findings underscore the ability of HSN-G1 to modulate a key neurotransmitter system implicated in Alzheimer's disease pathogenesis, and suggest that sex-specific mechanisms should be further explored to optimize therapeutic strategies. Further mechanistic investigation revealed sex-specific differences in cholinergic system components. Males demonstrated 34% lower AChE activity compared to females at the highest HSN-G1 dose (Table S3), which correlated with their higher ACh accumulation. Additionally, transporter expression analysis showed males had 28% higher CHT1 and 31% higher VAChT expression than females (Table S4), suggesting enhanced cholinergic efficiency.

3.5. Molecular mechanisms underlying HSN-G1 therapeutic effects

Western blot analyses revealed that HSN-G1 treatment modulated several key pathways implicated in Alzheimer’s disease pathology (Figs. 6 and 7). First, HSN-G1 significantly upregulated neurotrophic factors in both sexes. Notably, nerve growth factor (NGF) expression was particularly pronounced in male mice ($p < 0.001$), while brain-derived

neurotrophic factor (BDNF), ciliary neurotrophic factor (CNTF), and glial cell line-derived neurotrophic factor (GDNF) were consistently elevated in both males and females, suggesting a balanced neurotrophic support across sexes. Second, HSN-G1 exerted substantial effects on amyloid pathology through multiple clearance mechanisms. The treatment enhanced the expression of Aβ-clearing enzymes, including neprilysin (NEP) and insulin-degrading enzyme (IDE), and upregulated the scavenger receptor type A (SRA). This enhancement of clearance pathways resulted in significant reductions in brain Aβ42 levels, with a 63% decrease observed in female mice compared to a 48% reduction in males. Moreover, the amyloid-reducing efficacy of HSN-G1 surpassed that of donepezil, the current standard treatment. Third, analysis of cholinergic system modulation demonstrated dose-dependent increases in choline acetyltransferase (ChAT) expression and improved regulation of acetylcholine synthesis pathway components. In this regard, female mice exhibited significantly greater enhancements in cholinergic function ($p < 0.001$), which aligns with the sex-specific differences observed in other parameters. Collectively, the concurrent enhancement of neurotrophic support, amyloid clearance, and cholinergic function underscores the comprehensive therapeutic mechanisms of HSN-G1 in mitigating AD pathology. These findings suggest that HSN-G1 exerts its beneficial effects through a synergistic modulation of multiple molecular pathways, offering a promising multi-target approach for Alzheimer's disease treatment. These sex-specific differences in cholinergic metabolism were further

validated through comprehensive enzyme activity assays and transporter expression analyses (Tables S3-S4).

3.6. Comparative analysis of brain Aβ reduction

Immunohistochemical analysis revealed that HSN-G1 treatment significantly reduced Aβ deposition in both the cortical and hippocampal regions (Figs. 8A and 8B). These qualitative observations were corroborated by quantitative measurements using an enzyme-linked immunosorbent assay (ELISA), which showed approximately a 45% reduction in brain Aβ42 concentrations in both male and female APP/PS1 mice (Figs. 8C and 8D). Notably, the 400 mg/kg dose of HSN-G1 achieved a significantly greater reduction in Aβ levels than that observed with donepezil in both sexes ($p < 0.01$). The proposed mechanism of HSN-G1 is summarized in Fig. 9.

4. Discussion

In this comprehensive study, we demonstrated that HSN-G1, a novel ginsenoside-enriched formulation, effectively ameliorates cognitive deficits in APP/PS1 mice through multiple therapeutic mechanisms. Our results reveal several significant advances in AD therapeutics. First, we established an optimal ginsenoside ratio (Re/Rd/Rg3 = 33.27:25.00:12.18 mg/g) that not only maximizes therapeutic efficacy but also ensures pharmaceutical reproducibility, with a coefficient of variation (CV) of less than 3% (Ahn et al., 2021; Irfan et al., 2020; Lee & Kim, 2014). This high level of standardization overcomes a major challenge associated with

natural product-based drug development and provides a robust framework for future multi-target formulations.

Moreover, our investigation uncovered distinct sex-specific therapeutic responses. Male mice exhibited more stable and consistent cognitive improvements that were closely associated with enhanced NGF signaling (Eu et al., 2021; Gao et al., 2022; Kazim & Iqbal, 2016), whereas female mice showed a broader neurotrophic response and superior Aβ clearance (Ordóñez-Gutiérrez et al., 2015). These differences likely reflect complex interactions between sex hormones and AD pathophysiology, emphasizing the need for tailored dosing strategies in future clinical applications (Haywood & Mukaetova-Ladinska, 2006; Mielke, 2018).

Mechanistically, HSN-G1 exerts its effects by modulating several pathological pathways simultaneously. It enhances microglial Aβ clearance through SRA-dependent mechanisms and upregulates key Aβ-degrading enzymes, including neprilysin and IDE (Jang et al., 2015; Wilkinson & El Khoury, 2012). In addition, HSN-G1 improves cholinergic function, as evidenced by increased expression of ChAT and elevated acetylcholine levels (Chen et al., 2022; Mesulam, 2004). The concurrent upregulation of neurotrophic factors such as BDNF, NGF, CNTF, and GDNF further suggests that HSN-G1 may offer disease-modifying benefits that extend beyond symptomatic relief. Notably, when compared with the current standard treatment, donepezil, HSN-G1 provided superior cognitive enhancement, particularly in spatial memory tasks (Cummings et al., 2014;

Lane et al., 2018). The proposed multi-target mechanism of HSN-G1 is illustrated in Fig. 9.

The translational potential of HSN-G1 is further supported by several additional findings. Toxicological assessments revealed excellent tolerability up to doses of 800 mg/kg, with no evidence of organ toxicity or adverse behavioral effects. Body weight remained stable throughout the treatment period across all doses, contrasting with the significant weight loss observed with high-dose donepezil. Pharmacokinetic analyses demonstrated efficient brain penetration at clinically feasible doses, and significant efficacy was observed across a broad dose range (100–400 mg/kg) (Lane et al., 2018; Peng et al., 2023). These results, combined with the superior cognitive outcomes relative to donepezil, suggest that HSN-G1 holds promise as a multi-target therapeutic candidate for AD.

The multifaceted mechanisms and robust efficacy profile of HSN-G1 position it as a potential game-changer in the landscape of AD therapeutics. Current pharmaceutical approaches have largely followed a single-target paradigm, yielding modest clinical benefits that primarily address symptoms rather than disease progression. HSN-G1 represents a paradigm shift in this approach by simultaneously targeting multiple pathological cascades with a standardized natural product formulation. The convergence of enhanced amyloid clearance, improved cholinergic function, and upregulated neurotrophic support addresses the complex pathophysiology of AD in ways that conventional monotherapies cannot

achieve. Furthermore, the sex-specific efficacy profiles observed in our study open new possibilities for precision medicine approaches in AD treatment. Table 2 summarizes the comprehensive sex-specific therapeutic responses observed in our study, highlighting the complex interplay between behavioral, biochemical, and molecular outcomes across sexes. These differential responses underscore the necessity for personalized therapeutic approaches in AD treatment. As the field increasingly recognizes the limitations of uniform treatment strategies for a heterogeneous condition, HSN-G1's differential effects in males and females align with the emerging direction of personalized neurodegenerative disease management. These distinctive characteristics, combined with its favorable safety profile and superior efficacy compared to current standard treatments, suggest that HSN-G1 may fundamentally transform therapeutic strategies for AD, offering new hope for meaningful disease modification rather than merely symptomatic management.

The divergence between behavioral and biochemical outcomes across sexes reveals important insights into AD pathophysiology. While female mice showed superior Aβ clearance (63% vs 48% in males), male mice demonstrated better cognitive improvements. This apparent paradox aligns with clinical observations that Aβ burden doesn't always correlate with cognitive status (Jack et al., 2010; Jagust, 2016). Male mice achieved superior cognitive performance through enhanced NGF signaling (3.2-fold increase vs 1.8-fold in females, $p<0.05$) and greater cholinergic receptor sensitivity (muscarinic receptor density: 147% vs 123% of WT), suggesting

that neurotrophic mechanisms may compensate for less efficient Aβ clearance. Conversely, females showed more robust microglial activation (CD68 expression: 89% increase vs 64% in males) and enhanced SRA-mediated phagocytosis (92% vs 78% Aβ uptake in vitro) but potentially at the cost of increased neuroinflammation affecting cognition. These sex-specific differences likely reflect hormonal influences: estrogen receptor signaling may enhance microglial Aβ clearance in females while testosterone promotes neurotrophin-mediated cognitive resilience in males (Rettberg et al., 2014).

The paradoxical finding of higher ChAT expression in females but higher ACh levels in males reflects complex sex-specific differences in cholinergic dynamics. The observed 34% lower AChE activity in males explains their higher ACh accumulation despite lower synthesis, leading to ACh accumulation despite lower synthesis. Additionally, the enhanced expression of choline transporters (CHT1 and VAChT) in males contributes to their superior ACh utilization and storage efficiency, improving ACh utilization and storage efficiency. These differences likely reflect hormonal influences: estrogen enhances ChAT expression but also increases AChE activity in females, while testosterone reduces ACh degradation in males (Craig et al., 2011; Nakamura et al., 2002).

Despite these encouraging findings, several limitations must be acknowledged. First, our experiments were conducted using the APP/PS1 mouse model, which, although replicating key AD features (Malm et al.,

2011; Onos et al., 2019; Ordóñez-Gutiérrez et al., 2015), may not fully capture the heterogeneity of the human condition. Future studies should validate these results in additional animal models, such as the 3xTg-AD or tauopathy models. Second, while our 6-week treatment regimen produced significant benefits, longer-term studies are necessary to assess sustained efficacy and safety. Several limitations must be acknowledged. First, the small sample size is a major limitation that limits generalizability and statistical power, particularly for detecting subtle sex-specific differences. The observed treatment effects were consistent across individual animals, as demonstrated in the Results section. While we observed significant effects with high statistical significance, and individual animal data demonstrated consistent responses, these findings require validation in larger cohorts. (n=10-12/sex/group based on power analysis). The risk of Type II errors is substantial, and results should be interpreted cautiously. Second, analysis was limited to soluble Aβ fractions; brain pellets were not preserved for insoluble Aβ analysis, which represents a study limitation. Future studies will include comprehensive fractionation analysis of both soluble and insoluble Aβ species. Third, our 6-week treatment duration, while showing significant benefits, requires longer-term evaluation for chronic safety and sustained efficacy. Finally, although key molecular pathways were identified, further research is required to elucidate detailed interactions—including microglial phenotype transitions (Baek et al., 2018; Palasz et al., 2023; Wang et al., 2023) and potential epigenetic modifications.

In conclusion, our study establishes HSN-G1 as a significant advancement in AD therapeutics. Its standardized composition, multi-target mechanism of action, and observed sex-specific efficacy profiles collectively underscore its potential for clinical development. Future research should focus on optimizing dosing strategies, investigating long-term safety, and exploring combination therapies to fully realize the therapeutic potential of HSN-G1, paving the way for personalized treatment approaches in Alzheimer’s disease.

References

Ahn, J. W., Jang, S. K., Jo, B. R., Kim, H. S., Park, J. Y., Park, H. Y., Yoo, Y. M., & Joo, S. S. (2021). A therapeutic intervention for Alzheimer's disease using ginsenoside Rg3: its role in M2 microglial activation and non-amyloidogenesis. *J Physiol Pharmacol*, *72*(2). https://doi.org/10.26402/jpp.2021.2.04

Baek, J. Y., Jeong, J. Y., Kim, K. I., Won, S. Y., Chung, Y. C., Nam, J. H., Cho, E. J., Ahn, T. B., Bok, E., Shin, W. H., & Jin, B. K. (2018). Inhibition of microglia-derived oxidative stress by ciliary neurotrophic factor protects dopamine neurons *in vivo* from MPP^+ neurotoxicity. *Int J Mol Sci*, *19*(11). https://doi.org/10.3390/ijms19113543

Cao, G., Su, P., Zhang, S., Guo, L., Zhang, H., Liang, Y., Qin, C., & Zhang, W. (2016). Ginsenoside Re reduces Aβ production by activating PPARγ to inhibit BACE1 in N2a/APP695 cells. *Eur J Pharmacol*, *793*, 101-108. https://doi.org/10.1016/j.ejphar.2016.11.006

Carregosa, D., Carecho, R., Figueira, I., & C, N. S. (2020). Low-molecular weight metabolites from polyphenols as effectors for attenuating neuroinflammation. *J Agric Food Chem*, *68*(7), 1790-1807. https://doi.org/10.1021/acs.jafc.9b02155

Chen, Z.-R., Huang, J.-B., Yang, S.-L., & Hong, F.-F. (2022). Role of cholinergic signaling in Alzheimer's disease. *Molecules*, *27*(6), 1816. https://www.mdpi.com/1420-3049/27/6/1816

Craig, L. A., Hong, N. S., & McDonald, R. J. (2011). Revisiting the cholinergic hypothesis in the development of Alzheimer's disease. *Neuroscience & Biobehavioral Reviews*, *35*(6), 1397-1409. https://doi.org/https://doi.org/10.1016/j.neubiorev.2011.03.001

Cummings, J. L., Morstorf, T., & Zhong, K. (2014). Alzheimer's disease drug-development pipeline: few candidates, frequent failures. *Alzheimers Res Ther*, *6*(4), 37. https://doi.org/10.1186/alzrt269

Dong, H., Yuede, C. M., Coughlan, C. A., Murphy, K. M., & Csernansky, J. G. (2009). Effects of donepezil on amyloid-beta and synapse density in the Tg2576 mouse model of Alzheimer's disease. *Brain Res*, *1303*, 169-178. https://doi.org/10.1016/j.brainres.2009.09.097

Dong, Y., Li, X., Cheng, J., & Hou, L. (2019). Drug development for Alzheimer's disease: microglia induced neuroinflammation as a target? *Int J Mol Sci*, *20*(3).

Ellman, G. L., Courtney, K. D., Andres, V., & Featherstone, R. M. (1961). A new and rapid colorimetric determination of acetylcholinesterase activity. *Biochemical pharmacology*, *7*(2), 88-95. https://doi.org/https://doi.org/10.1016/0006-2952(61)90145-9

Eu, W. Z., Chen, Y.-J., Chen, W.-T., Wu, K.-Y., Tsai, C.-Y., Cheng, S.-J., Carter, R. N., & Huang, G.-J. (2021). The effect of nerve growth factor on supporting spatial memory depends upon hippocampal cholinergic innervation. *Translational psychiatry*, *11*(1), 162. https://doi.org/10.1038/s41398-021-01280-3

Fang, F., Chen, X., Huang, T., Lue, L. F., Luddy, J. S., & Yan, S. S. (2012).

Multi-faced neuroprotective effects of Ginsenoside Rg1 in an Alzheimer mouse model. *Biochim Biophys Acta*, *1822*(2), 286-292. https://doi.org/10.1016/j.bbadis.2011.10.004

Gao, L., Zhang, Y., Sterling, K., & Song, W. (2022). Brain-derived neurotrophic factor in Alzheimer's disease and its pharmaceutical potential. *Transl Neurodegener*, *11*(1), 4. https://doi.org/10.1186/s40035-022-00279-0

Gaugler, J. E., Yu, F., Davila, H. W., & Shippee, T. (2014). Alzheimer's disease and nursing homes. *Health Aff (Millwood)*, *33*(4), 650-657. https://doi.org/10.1377/hlthaff.2013.1268

Guo, T., Zhang, D., Zeng, Y., Huang, T. Y., Xu, H., & Zhao, Y. (2020). Molecular and cellular mechanisms underlying the pathogenesis of Alzheimer's disease. *Mol Neurodegener*, *15*(1), 40. https://doi.org/10.1186/s13024-020-00391-7

Haywood, W. M., & Mukaetova-Ladinska, E. B. (2006). Sex influences on cholinesterase inhibitor treatment in elderly individuals with Alzheimer's disease. *Am J Geriatr Pharmacother*, *4*(3), 273-286. https://doi.org/10.1016/j.amjopharm.2006.09.009

Irfan, M., Kim, M., & Rhee, M. H. (2020). Anti-platelet role of Korean ginseng and ginsenosides in cardiovascular diseases. *J Ginseng Res*, *44*(1), 24-32. https://doi.org/10.1016/j.jgr.2019.05.005

Jack, C. R., Jr., Knopman, D. S., Jagust, W. J., Shaw, L. M., Aisen, P. S., Weiner, M. W., Petersen, R. C., & Trojanowski, J. Q. (2010). Hypothetical model of dynamic biomarkers of the Alzheimer's pathological cascade. *Lancet Neurol*, *9*(1), 119-128. https://doi.org/10.1016/s1474-4422(09)70299-6

Jackson, H. M., Soto, I., Graham, L. C., Carter, G. W., & Howell, G. R. (2013). Clustering of transcriptional profiles identifies changes to insulin signaling as an early event in a mouse model of Alzheimer's disease. *BMC Genomics*, *14*, 831. https://doi.org/10.1186/1471-2164-14-831

Jagust, W. (2016). Is amyloid-β harmful to the brain? Insights from human imaging studies. *Brain*, *139*(Pt 1), 23-30. https://doi.org/10.1093/brain/awv326

Jang, S. K., Yu, J. M., Kim, S. T., Kim, G. H., Park, D. W., Lee, D. I., & Joo, S. S. (2015). An Aβ42 uptake and degradation via Rg3 requires an activation of caveolin, clathrin and Aβ-degrading enzymes in microglia. *Eur J Pharmacol*, *758*, 1-10. https://doi.org/10.1016/j.ejphar.2015.03.071

Jiang, T., Yu, J. T., & Tan, L. (2012). Novel disease-modifying therapies for Alzheimer's disease. *J Alzheimers Dis*, *31*(3), 475-492. https://doi.org/10.3233/jad-2012-120640

Kazim, S. F., & Iqbal, K. (2016). Neurotrophic factor small-molecule mimetics mediated neuroregeneration and synaptic repair: emerging therapeutic modality for Alzheimer's disease. *Mol Neurodegener*, *11*(1), 50. https://doi.org/10.1186/s13024-016-0119-y

Klein, W. L., Krafft, G. A., & Finch, C. E. (2001). Targeting small Aβ oligomers: the solution to an Alzheimer's disease conundrum? *Trends in Neurosciences*, *24*(4), 219-224. https://doi.org/https://doi.org/10.1016/S0166-2236(00)01749-5

Lane, C. A., Hardy, J., & Schott, J. M. (2018). Alzheimer's disease. *Eur J Neurol*, *25*(1), 59-70. https://doi.org/https://doi.org/10.1111/ene.13439

Lee, C. H., & Kim, J. H. (2014). A review on the medicinal potentials of ginseng and ginsenosides on cardiovascular diseases. *J Ginseng Res*, *38*(3), 161-166. https://doi.org/10.1016/j.jgr.2014.03.001

Malm, T., Koistinaho, J., & Kanninen, K. (2011). Utilization of APPswe/PS1dE9 transgenic mice in research of Alzheimer's disease: Focus on gene therapy and cell-based therapy applications. *Int J Alzheimers Dis*, *2011*, 517160. https://doi.org/10.4061/2011/517160

Mesulam, M. (2004). The cholinergic lesion of Alzheimer's disease: pivotal factor or side show? *Learn Mem*, *11*(1), 43-49. https://doi.org/10.1101/lm.69204

Mielke, M. M. (2018). Sex and gender differences in Alzheimer's disease dementia. *Psychiatr Times*, *35*(11), 14-17.

Minkeviciene, R., Ihalainen, J., Malm, T., Matilainen, O., Keksa-Goldsteine, V., Goldsteins, G., Iivonen, H., Leguit, N., Glennon, J., Koistinaho, J., Banerjee, P., & Tanila, H. (2008). Age-related decrease in stimulated glutamate release and vesicular glutamate transporters in APP/PS1 transgenic and wild-type mice. *J Neurochem*, *105*(3), 584-594. https://doi.org/10.1111/j.1471-4159.2007.05147.x

Nakamura, N., Fujita, H., & Kawata, M. (2002). Effects of gonadectomy on immunoreactivity for choline acetyltransferase in the cortex, hippocampus, and basal forebrain of adult male rats. *Neuroscience*, *109*(3), 473-485. https://doi.org/10.1016/s0306-4522(01)00513-9

Onos, K. D., Uyar, A., Keezer, K. J., Jackson, H. M., Preuss, C., Acklin, C. J., O'Rourke, R., Buchanan, R., Cossette, T. L., Sukoff Rizzo, S. J., Soto, I., Carter, G. W., & Howell, G. R. (2019). Enhancing face validity of mouse models of Alzheimer's disease with natural genetic variation. *PLoS Genet*, *15*(5), e1008155. https://doi.org/10.1371/journal.pgen.1008155

Ordóñez-Gutiérrez, L., Re, F., Bereczki, E., Ioja, E., Gregori, M., Andersen, A. J., Antón, M., Moghimi, S. M., Pei, J. J., Masserini, M., & Wandosell, F. (2015). Repeated intraperitoneal injections of liposomes containing phosphatidic acid and cardiolipin reduce amyloid-β levels in APP/PS1 transgenic mice. *Nanomedicine*, *11*(2), 421-430. https://doi.org/10.1016/j.nano.2014.09.015

Paik, S., Song, G. Y., & Jo, E. K. (2023). Ginsenosides for therapeutically targeting inflammation through modulation of oxidative stress. *Int Immunopharmacol*, *121*, 110461. https://doi.org/10.1016/j.intimp.2023.110461

Palasz, E., Wilkaniec, A., Stanaszek, L., Andrzejewska, A., & Adamczyk, A. (2023). Glia-neurotrophic factor relationships: possible role in

pathobiology of neuroinflammation-related brain disorders. *Int J Mol Sci*, *24*(7).

Park, D., Choi, E. K., Cho, T. H., Joo, S. S., & Kim, Y. B. (2020). Human neural stem cells encoding ChAT gene restore cognitive function via acetylcholine synthesis, Aβ elimination, and beuroregeneration in APPswe/PS1dE9 mice. *Int J Mol Sci*, *21*(11). https://doi.org/10.3390/ijms21113958

Passeri, E., Elkhoury, K., Morsink, M., Broersen, K., Linder, M., Tamayol, A., Malaplate, C., Yen, F. T., & Arab-Tehrany, E. (2022). Alzheimer's disease: treatment strategies and their limitations. *Int J Mol Sci*, *23*(22). https://doi.org/10.3390/ijms232213954

Peng, Y., Jin, H., Xue, Y. H., Chen, Q., Yao, S. Y., Du, M. Q., & Liu, S. (2023). Current and future therapeutic strategies for Alzheimer's disease: an overview of drug development bottlenecks. *Front Aging Neurosci*, *15*, 1206572. https://doi.org/10.3389/fnagi.2023.1206572

Phan, H. T. T., Samarat, K., Takamura, Y., Azo-Oussou, A. F., Nakazono, Y., & Vestergaard, M. C. (2019). Polyphenols modulate Alzheimer's amyloid beta aggregation in a structure-dependent manner. *Nutrients*, *11*(4). https://doi.org/10.3390/nu11040756

Rahman, A., Jackson, H., Hristov, H., Isaacson, R. S., Saif, N., Shetty, T., Etingin, O., Henchcliffe, C., Brinton, R. D., & Mosconi, L. (2019). Sex and gender driven modifiers of Alzheimer's: The role for estrogenic control across age, race, medical, and lifestyle risks [Review]. *Front Aging Neurosci*, *11*. https://doi.org/10.3389/fnagi.2019.00315

Rettberg, J. R., Yao, J., & Brinton, R. D. (2014). Estrogen: a master regulator of bioenergetic systems in the brain and body. *Front Neuroendocrinol*, *35*(1), 8-30. https://doi.org/10.1016/j.yfrne.2013.08.001

Sun, B. L., Li, W. W., Zhu, C., Jin, W. S., Zeng, F., Liu, Y. H., Bu, X. L., Zhu, J., Yao, X. Q., & Wang, Y. J. (2018). Clinical research on Alzheimer's disease: progress and perspectives. *Neurosci Bull*, *34*(6), 1111-1118. https://doi.org/10.1007/s12264-018-0249-z

Szwajgier, D., Borowiec, K., & Pustelniak, K. (2017). The neuroprotective effects of phenolic acids: Molecular mechanism of action. *Nutrients*, *9*(5). https://doi.org/10.3390/nu9050477

Takada-Takatori, Y., Nakagawa, S., Kimata, R., Nao, Y., Mizukawa, Y., Urushidani, T., Izumi, Y., Akaike, A., Tsuchida, K., & Kume, T. (2019). Donepezil modulates amyloid precursor protein endocytosis and reduction by up-regulation of SNX33 expression in primary cortical neurons. *Sci Rep*, *9*(1), 11922. https://doi.org/10.1038/s41598-019-47462-4

Thapa, A., & Carroll, N. J. (2017). Dietary modulation of oxidative stress in Alzheimer's disease. *Int J Mol Sci*, *18*(7), 1583. https://www.mdpi.com/1422-0067/18/7/1583

Wang, C., Zong, S., Cui, X., Wang, X., Wu, S., Wang, L., Liu, Y., & Lu, Z. (2023). The effects of microglia-associated neuroinflammation on Alzheimer's disease. *Front Immunol*, *14*, 1117172.

https://doi.org/10.3389/fimmu.2023.1117172

Waters, A., & Laitner, M. H. (2021). Biological sex differences in Alzheimer's preclinical research: A call to action. *Alzheimers Dement (N Y)*, *7*(1), e12111. https://doi.org/10.1002/trc2.12111

Wilkinson, K., & El Khoury, J. (2012). Microglial scavenger receptors and their roles in the pathogenesis of Alzheimer's disease. *Int J Alzheimers Dis*, *2012*, 489456. https://doi.org/10.1155/2012/489456

Yang, X., Chu, S. F., Wang, Z. Z., Li, F. F., Yuan, Y. H., & Chen, N. H. (2021). Ginsenoside Rg1 exerts neuroprotective effects in 3-nitropronpionic acid-induced mouse model of Huntington's disease via suppressing MAPKs and NF-κB pathways in the striatum. *Acta Pharmacol Sin*, *42*(9), 1409-1421. https://doi.org/10.1038/s41401-020-00558-4

Yoon, E.-J., Ahn, J.-W., Kim, H.-S., Choi, Y., Jeong, J., Joo, S.-S., & Park, D. (2023). Improvement of cognitive function by fermented *Panax ginseng* C.A. Meyer berries extracts in an AF64A-induced memory deficit model. *Nutrients*, *15*(15), 3389. https://www.mdpi.com/2072-6643/15/15/3389

Zhang, H., Su, Y., Sun, Z., Chen, M., Han, Y., Li, Y., Dong, X., Ding, S., Fang, Z., Li, W., & Li, W. (2021). Ginsenoside Rg1 alleviates Aβ deposition by inhibiting NADPH oxidase 2 activation in APP/PS1 mice. *J Ginseng Res*, *45*(6), 665-675. https://doi.org/10.1016/j.jgr.2021.03.003

Zhang, Y., Chen, H., Li, R., Sterling, K., & Song, W. (2023). Amyloid β-based therapy for Alzheimer's disease: challenges, successes and future. *Signal Transduct Target Ther*, *8*(1), 248. https://doi.org/10.1038/s41392-023-01484-7

Acknowledgements

This research was supported by the Korea Health Technology R&D Project through the Korea Health Industry Development Institute (KHIDI) and Korea Dementia Research Center (KDRC), funded by the Ministry of Health & Welfare and the Ministry of Science and ICT, Republic of Korea (grant number: HU21C0332).

Author contributions

Jeong Won Ahn: Data curation, methodology, visualization, writing—original draft

Eun-Jung Yoon: Data curation, formal analysis, visualization, writing—original draft

Hyun Soo Kim: Formal analysis, validation

Yunseo Choi: Methodology, software

Jiwon Jeong: Methodology, validation

Kongara Damodar: Investigation, software

Yeong-Min Yoo: Project administration, writing—review and editing

Dongsun Park: Conceptualization, data curation, project administration, supervision, writing—review and editing

Seong Soo Joo: Conceptualization, funding acquisition, supervision, writing—review and editing

Data availability statement

The original contributions presented in the study are included in the article/Supplementary Material, further inquiries can be directed to the corresponding author.

Ethics approval statement

All animal experiments were conducted in accordance with the Standard Operation Procedures of the Laboratory Animal Center at Chungbuk National University, Republic of Korea. The protocol was approved by the Institutional Animal Care and Use Committee of CBNU (#CBNUA-1398-20-01).

Conflict of interest

The authors have declared no conflict of interest.

Abbreviations

AD, Alzheimer's disease; Aβ, amyloid-beta; APP/PS1, APPswe/PS1dE9; HPLC, high-performance liquid chromatography; LDH, lactate dehydrogenase; SRA, scavenger receptor type A; PAT, passive avoidance test; MWMT, Morris water maze test; ACh, acetylcholine; GFAP, glial fibrillary acidic protein; BDNF, brain-derived neurotrophic factor; NGF, nerve growth factor; CNTF, ciliary neurotrophic factor; GDNF, glial cell line-derived neurotrophic factor; ChAT, choline acetyltransferase; NEP, neprilysin; IDE, insulin-degrading enzyme; CHT, choline transporter; VAChT, vesicular acetylcholine transporter

Figure legends

Fig. 1. Schematic illustration of the *in vivo* study design. (A) Experimental timeline and group allocation. APP/PS1 and wild-type (WT) mice (n = 6 per group, equal numbers of males and females) received oral administration of vehicle (saline), donepezil (2 mg/kg/day), or HSN-G1 (100, 200, or 400 mg/kg/day) for six weeks. Memory function was assessed using behavioral tests during week 5, followed by tissue collection in week 6. (B and C) Schematic representations of behavioral paradigms: (B) passive avoidance test for associative memory assessment and (C) Morris water maze test for spatial memory evaluation.

Fig. 2. A representative HPLC chromatogram of HSN-G1, showing the separation of ginsenosides using a YMC-Triart C18 column (250 × 4.6 mm, 5 µm) at 30°C with detection at 203 nm. Peak identification was performed by comparing the retention times and UV spectra with those of standard ginsenosides. The numbered peaks correspond to: Rg1 (1), Re (2), Rb1 (3), Rc (4), Rb2 (5), F1 (6), Rd (7), F4 (8), F2 (9), Rg3(S) (10), Rg3(R) (11), Rk1 (12), Rg5 (13), CK (14), and Rh2 (15). Quantitative analysis for each component is presented in Table 1. Data represent three independent analyses, demonstrating consistent reproducibility.

Fig. 3. Fig. 3. Effect of HSN-G1 on amyloid-beta (Aβ) clearance and neuroprotection. (A) Cell viability was assessed using a lactate dehydrogenase (LDH) assay in human microglial HMO6 cells and scavenger receptor A-overexpressing HMO6 cells (HMO6.SRA). Cells were

pretreated with HSN-G1 (100, 200, or 400 μg/mL) or donepezil (1 μM) for 30 min, followed by exposure to Aβ42 (5 μM) for 4 h. (B) Representative fluorescence microscopy images of Aβ-FITC clearance in HMO6 and HMO6.SRA cells. Images were captured after 24 h of treatment under identical exposure conditions (scale bar = 50 μm). (C) Quantitative analysis of fluorescence intensity from panel B. Fluorescence intensity was measured using ImageJ software from five random fields per condition and normalized to Aβ42 control (100%). HMO6.SRA cells exhibited significantly enhanced Aβ clearance compared to HMO6 cells, with 92% reduction in intracellular FITC-Aβ levels at 400 μg/mL HSN-G1. Data represent means ± SD from three independent experiments. #p < 0.05, ##p < 0.01, ###p < 0.001 versus Aβ42 treatment alone.

Fig. 4. Assessment of cognitive function in APP/PS1 mice following HSN-G1 treatment. (A and B) Passive avoidance test (PAT) results showing step-through latency in female (A) and male (B) mice. (C and D) Morris water maze test (MWMT) performance in female (C) and male (D) mice, conducted during week 5 of treatment. APP/PS1 and wild-type (WT) mice (n = 6 per group, with equal numbers of males and females) received oral administration (via gavage) of vehicle (saline), donepezil (2 mg/kg/day), or HSN-G1 (100, 200, or 400 mg/kg/day) for 6 weeks. Male mice demonstrated more stable and consistent improvements in both tests, particularly in spatial memory performance. For the PAT, a cutoff time of 180 s was applied for mice that remained in the illuminated chamber. For the MWMT, platform-finding was limited to 180 s per trial, with four trials

conducted daily over 5 consecutive days. Data are presented as means ± SD. $p < 0.05$, ** p < 0.01, *** $p < 0.001$ versus WT control; # $p < 0.05$, ## $p < 0.01$, ### $p < 0.001$ versus vehicle-treated APP/PS1 mice.

Fig. 5. Effects of HSN-G1 on brain acetylcholine (ACh) concentrations. (A and B) Brain tissue ACh levels in female (A) and male (B) mice were quantified using the Amplex Red Acetylcholine/Acetylcholinesterase Assay Kit. Male mice showed a 73% increase, while female mice exhibited a 55% increase in ACh levels at the 400 mg/kg dose of HSN-G1. Brain tissues were collected after 6 weeks of treatment with vehicle (saline), donepezil (2 mg/kg/day), or HSN-G1 (100, 200, or 400 mg/kg/day). Samples were homogenized in PBS containing protease inhibitors, and ACh levels were normalized to total protein content. Data represent means ± SD from three independent experiments (n = 3 per group). ***$p < 0.001$ versus WT control; #p < 0.05, ###$p < 0.001$ versus vehicle-treated APP/PS1 mice.

Fig. 6. Effect of HSN-G1 on neurotrophic and amyloid pathology-related protein expression in female APP/PS1 mice. (A) Representative Western blot images showing the modulation of neurotrophic factors (BDNF, NGF, CNTF, and GDNF) and Aβ-clearance proteins (NEP, IDE, and SRA) in female APP/PS1 mice following treatment with vehicle (saline), donepezil (2 mg/kg), or HSN-G1 (100, 200, and 400 mg/kg). (B and C) Quantitative analysis of protein expression levels, normalized to GAPDH and expressed as fold change relative to wild-type controls. HSN-G1 treatment consistently elevated both neurotrophic factors and Aβ-clearance proteins.

Statistical significance: *$p < 0.05$, **$p < 0.01$, ***$p < 0.001$ versus WT; #$p < 0.05$, ##$p < 0.01$, ###$p < 0.001$ versus vehicle-treated APP/PS1 mice. Data represent mean ± SD (n = 3 per group).

Fig. 7. Effects of HSN-G1 on neurotrophic factor expression and amyloid-related proteins in male APP/PS1 mice. (A) Representative Western blot images demonstrating the effects of HSN-G1 on key growth factors (BDNF, NGF, CNTF, and GDNF) and Aβ-related proteins (NEP, IDE, and SRA) in male APP/PS1 mice. Notably, NGF expression was markedly increased in male mice following HSN-G1 treatment. Treatment groups included vehicle, donepezil (2 mg/kg), and HSN-G1 at doses of 100, 200, and 400 mg/kg. (B and C) Quantitative analysis of protein expression levels, normalized to GAPDH and expressed as fold change relative to wild-type controls. Statistical significance: *$p < 0.05$, **$p < 0.01$, ***$p < 0.001$ versus WT; #$p < 0.05$, ##$p < 0.01$, ###$p < 0.001$ versus vehicle-treated APP/PS1 mice. Data are presented as mean ± SD (n = 3 per group).

Fig. 8. Comparative analysis of amyloid-beta deposition in APP/PS1 mice treated with HSN-G1 and donepezil. (A, B) Immunohistochemical staining of coronal brain sections from female (A) and male (B) mice, illustrating Aβ plaque accumulation in the cortical and hippocampal regions. Scale bar = 500 μm. (C, D) Quantitative analysis of soluble Aβ42 levels by ELISA in female (C) and male (D) mice, showing an approximate 45% reduction in both sexes following HSN-G1 treatment. Data are expressed as mean ± SD (n = 3 per group). Notably, HSN-G1, particularly at the 400 mg/kg dose,

demonstrated superior Aβ reduction compared to donepezil. Statistical significance: $^{**}p < 0.01$, $^{***}p < 0.001$ versus WT; $\#p < 0.05$, $\#\#p < 0.01$ versus vehicle-treated APP/PS1 mice.

Fig. 9. Proposed mechanism of HSN-G1 in Alzheimer's disease. HSN-G1 (ginsenoside Re/Rd/Rg3 formulation) exerts therapeutic effects through three complementary pathways: microglial Aβ clearance via SRA/NEP/IDE upregulation (enhanced in females), cholinergic function improvement through ChAT upregulation and AChE inhibition (enhanced in males), and neurotrophic support via BDNF, NGF, CNTF, and GDNF upregulation. These multi-target mechanisms converge to reduce brain Aβ burden (~45%) and improve cognitive function, representing a therapeutic advantage over single-target approaches such as donepezil. SRA, scavenger receptor A; NEP, neprilysin; IDE, insulin-degrading enzyme; ChAT, choline acetyltransferase; AChE, acetylcholinesterase; BDNF, brain-derived neurotrophic factor; NGF, nerve growth factor; CNTF, ciliary neurotrophic factor; GDNF, glial cell line-derived neurotrophic factor.

Figures

Fig. 1

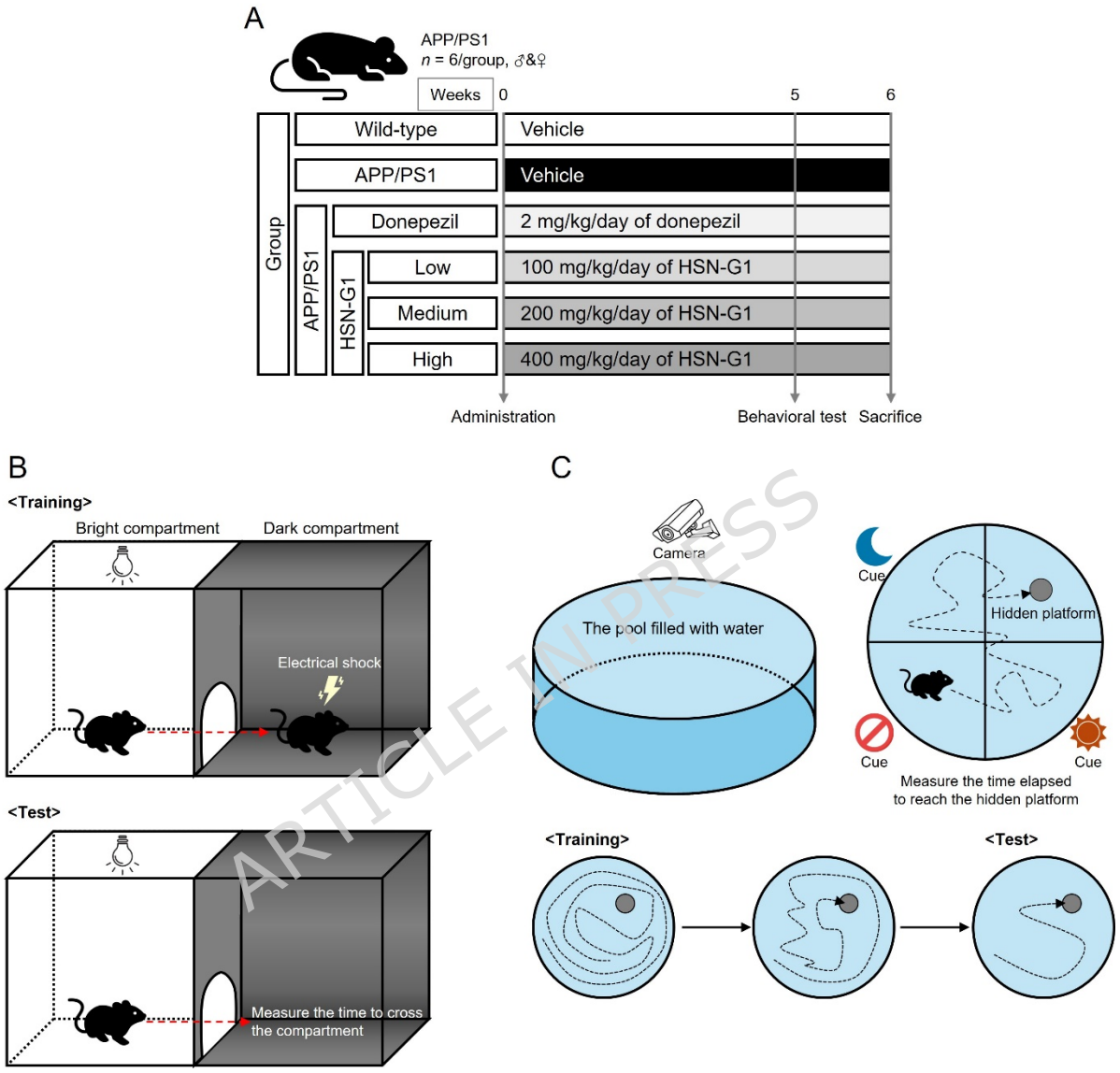

Fig. 2

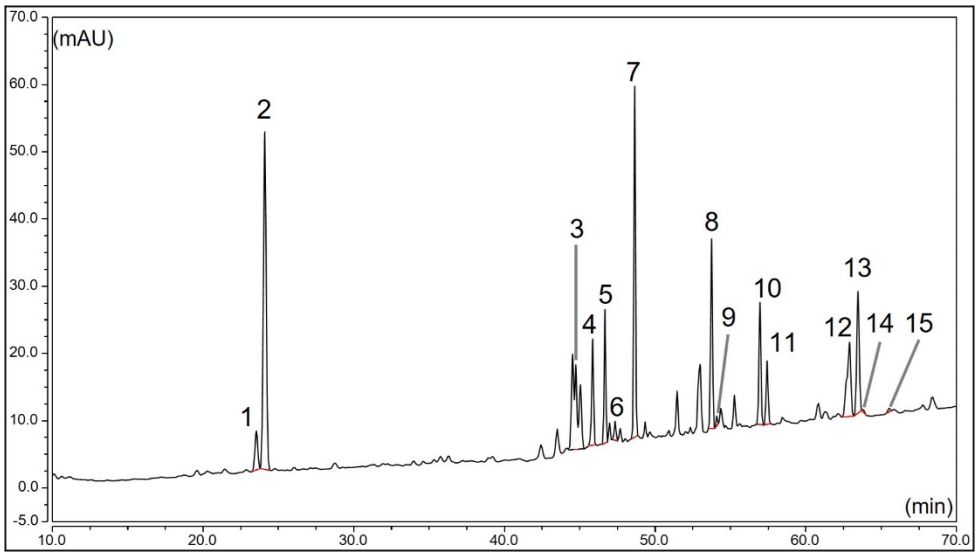

Fig. 3

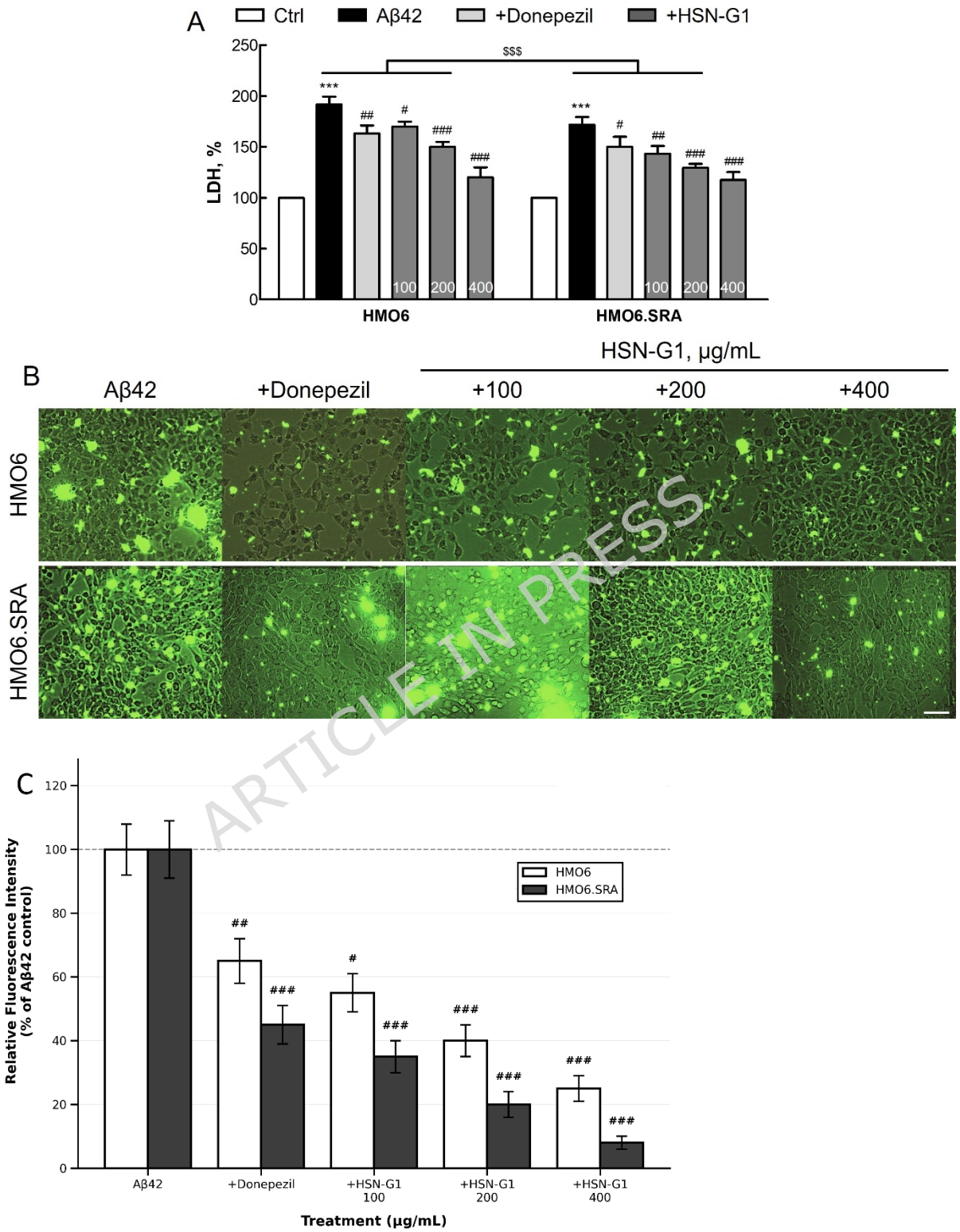

Fig. 4

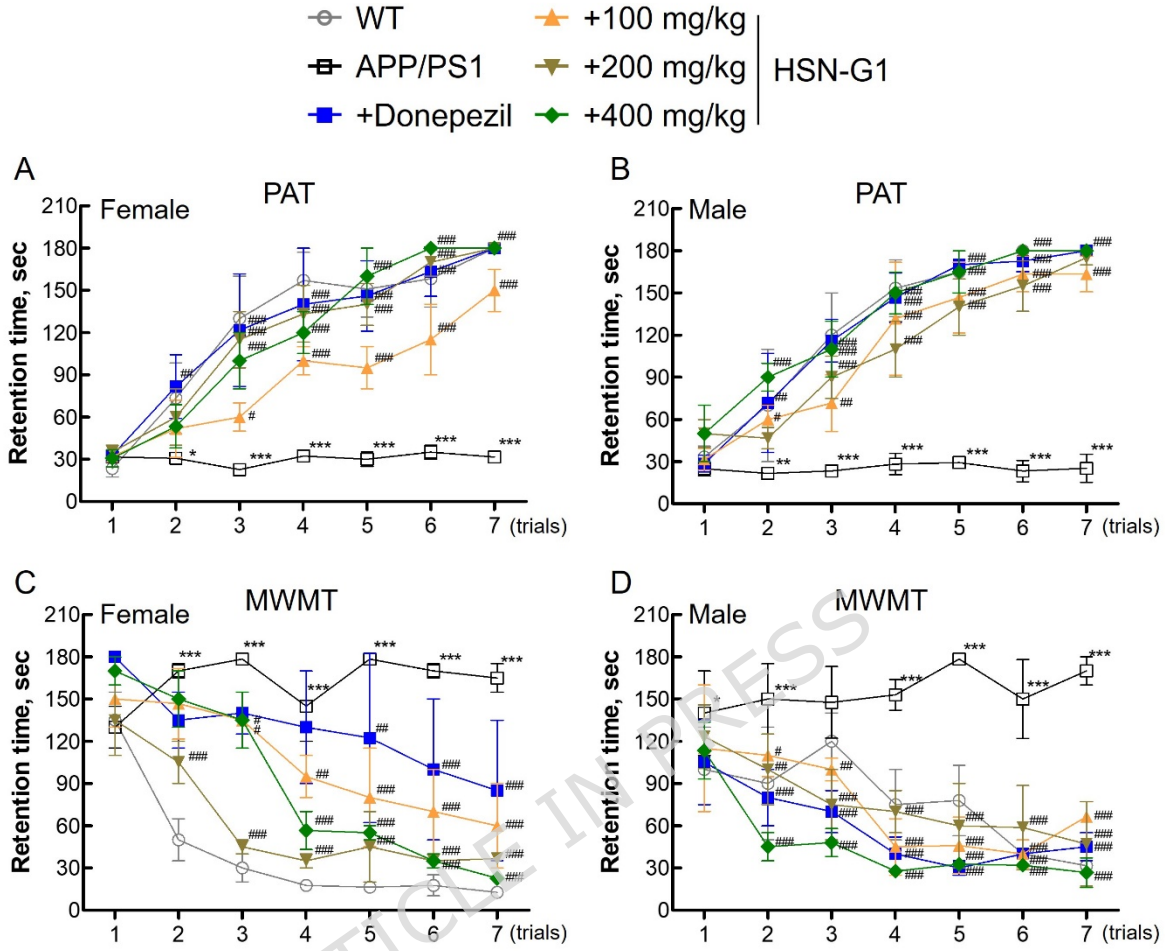

Fig. 5

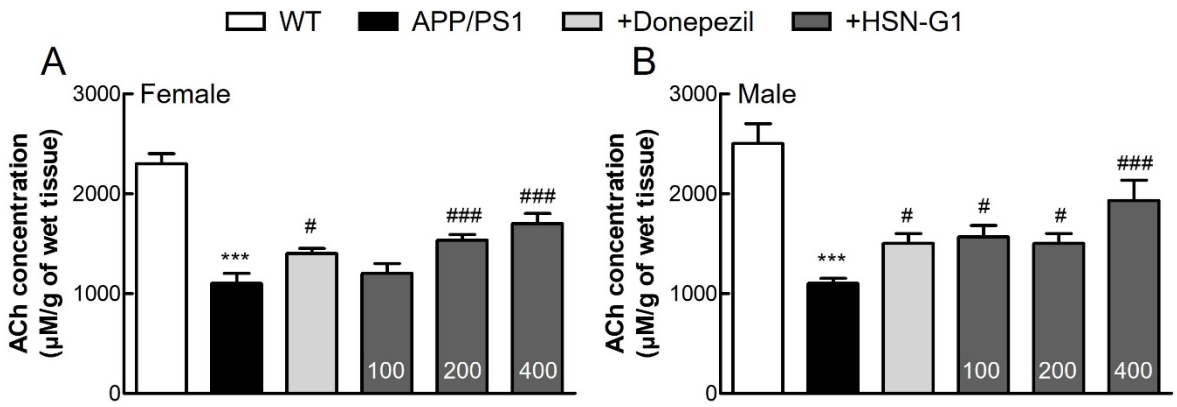

Fig. 6

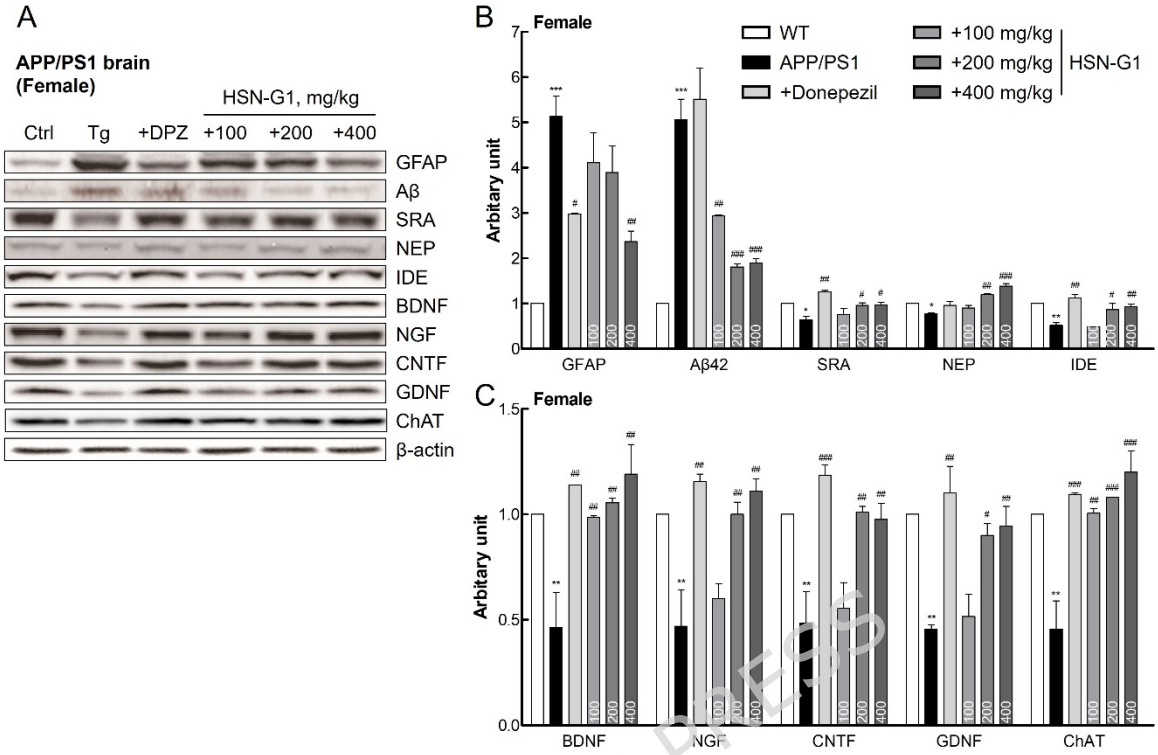

Fig. 7

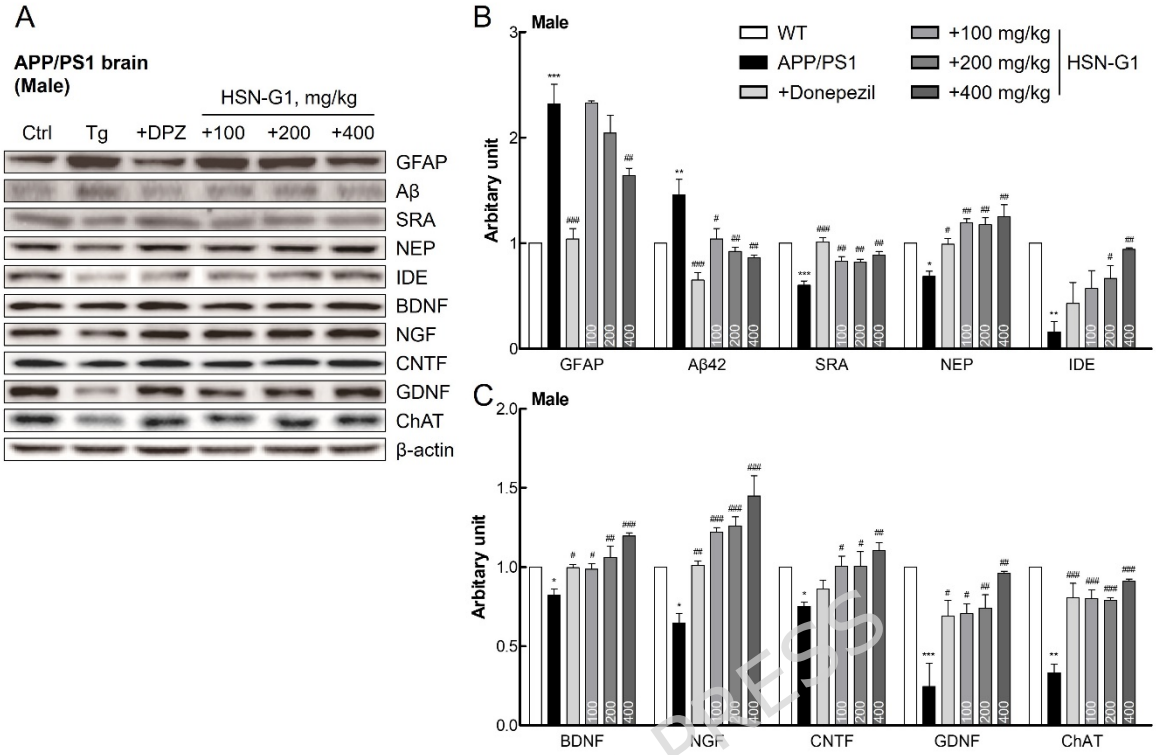

Fig. 8

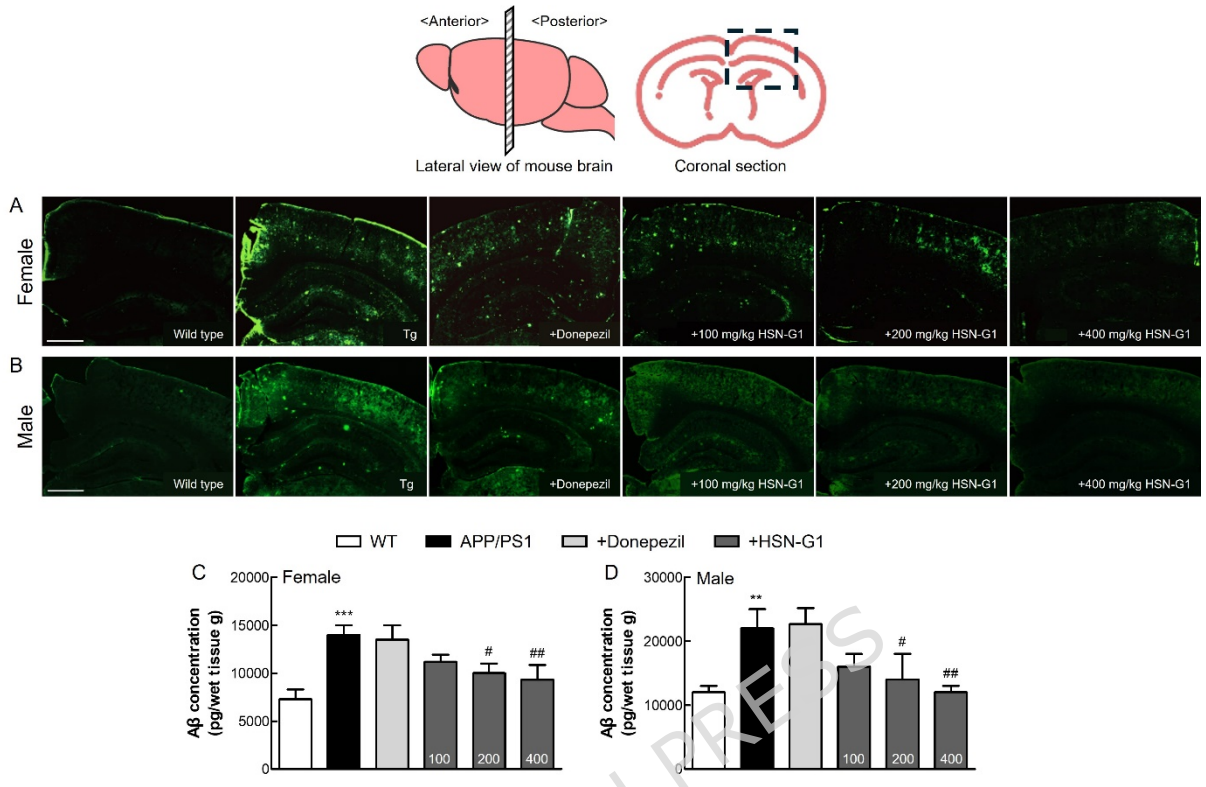

Fig. 9

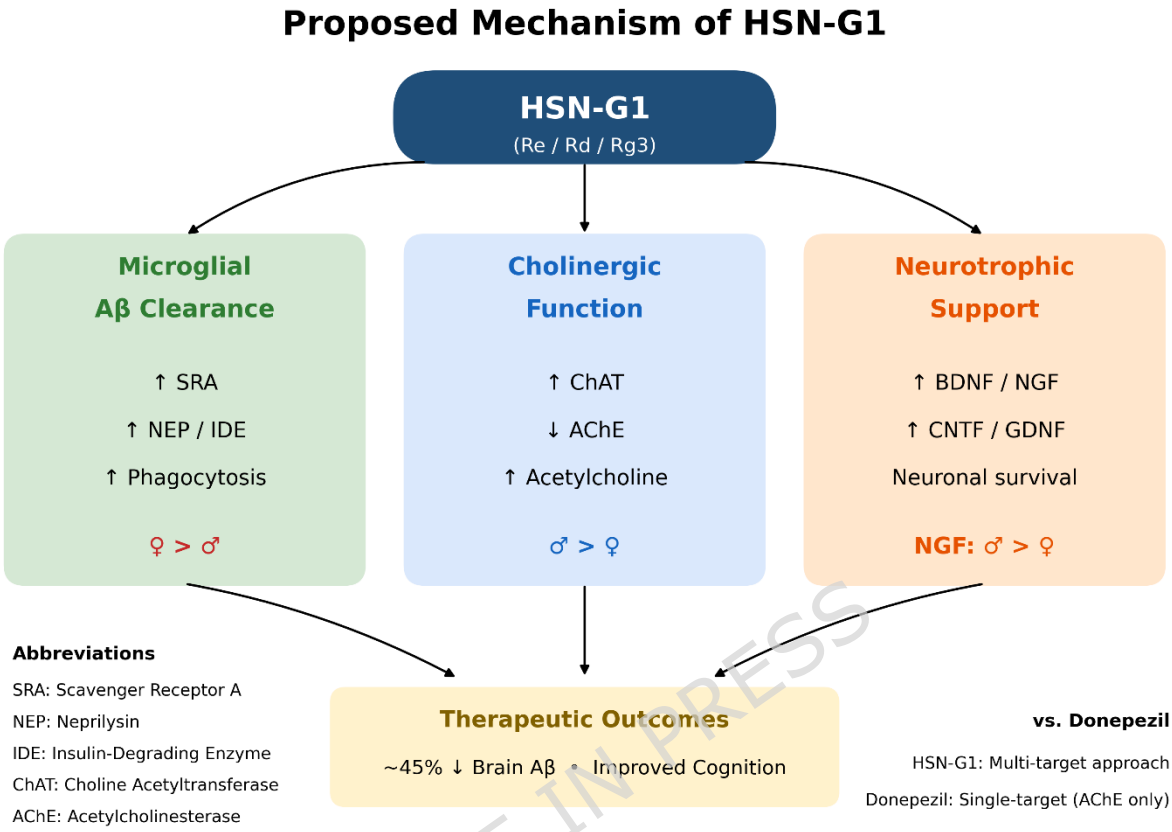

Table

Table 1. Quantitative analysis of the ginsenoside composition of HSN-G1

Peak #	Name	RT (min)	Area (mAU*min)	Relative area %	Amount (mg/g)
1	Rg1	23.53	1.25	3.01	2.40 ± 0.13
2	Re	24.09	11.06	26.73	33.27 ± 0.35
3	Rb1	44.73	1.99	4.81	7.28 ± 0.17
4	Rc	45.85	2.29	5.53	6.71 ± 0.15
5	Rb2	46.67	2.50	6.04	9.39 ± 0.20
6	F1	47.34	0.40	0.97	0.73 ± 0.08
7	Rd	48.64	6.54	15.82	25.00 ± 0.29
8	F4	53.74	4.09	9.87	9.20 ± 0.11
9	F2	54.09	0.17	0.41	0.41 ± 0.02
10	Rg3(S)	56.95	2.74	6.62	8.14 ± 0.12
11	Rg3(R)	57.42	1.47	3.55	4.04 ± 0.09
12	Rk1	62.89	3.27	7.91	3.28 ± 0.10
13	Rg5	63.45	3.44	8.30	2.76 ± 0.08
14	CK	63.81	0.07	0.17	0.12 ± 0.01
15	Rh2	65.53	0.10	0.25	0.14 ± 0.01

Table 2. Summary of sex-specific therapeutic responses to HSN-G1 treatment

Parameter	Males	Females	Proposed Mechanism
Cognitive improvement	+++	++	Enhanced NGF/cholinergic signaling in males
Aβ clearance	++ (48%)	+++ (63%)	Greater microglial activation in females
ACh levels	+++ (73%)	++ (55%)	Lower AChE activity in males
ChAT expression	++	+++	Estrogen-mediated upregulation
NGF expression	+++	++	Testosterone-dependent regulation
Behavioral consistency	High	Moderate	Superior compensatory mechanisms in males